

# Real-Time Power Market Clearing Model with Improved Network Constraints Considering PTDF Correction and Fast-Calculated Dynamic Line Rating

**Pan, Hongyu; Chen, Xinyu; Jin, Tianyu; Bai, Yang; Chen, Zhongfei; Wen, Jinyu; Wu, Qiuwei**

*Published in:*
IEEE Transactions on Industry Applications

*Link to article, DOI:*
10.1109/TIA.2022.3218271

*Publication date:*
2023

*Document Version*
Peer reviewed version

# Real-Time Power Market Clearing Model with Improved Network Constraints Considering PTDF Correction and Fast-Calculated Dynamic Line Rating

Hongyu Pan, Xinyu Chen, *Member*, *IEEE*, Tianyu Jin, *Student Member*, *IEEE*, Yang Bai, Zhongfei Chen, Jinyu Wen, *Member*, *IEEE*, and Qiuwei Wu, *Senior Member*, *IEEE*

***Abstract*—The increasing penetration of renewables in power systems reconfigures the generation mix and geography distribution, resulting in more frequent power flow congestion. Conventionally, a relatively conservative dispatch margin for transmission congestion in network constraints was reserved to ensure safe operation due to potential deviations introduced by DC power flow modeling and conservative line rating. This paper proposes a real-time power market clearing model with improved network constraints considering power transfer distribution factor (PTDF) correction and fast-calculated dynamic line rating. The clearing model based on PTDF correction is proposed first employing the Taylor expansion with the voltage and phase angle approximation. An improved dynamic line rating model is further applied into the clearing model based on the piecewise linear approximation method, which calculates real-time conductor temperature faster with sufficient precision. We test and verify the validity of the proposed model based on three independent systems including the IEEE 39-bus system, the IEEE 2383-bus system, and the real power grid system in Yunnan province of China, respectively. The results show that the improved clearing model reduces the calculated power flow deviation between the clearing results and real conditions compared with traditional security constraints, where the efficiency of power grid operation is also increased.**

***Index Terms*—Real-time market, network constraints, PTDF correction, dynamic line rating**

## I. Introduction

The generation mix and geographical distribution have been reconfigured gradually in power systems with the increasing penetration of renewables [1]. Thus, the original power equilibrium in the network will be changed, resulting in unbalanced power flow distribution with more frequent congestion. The risk of power flow overload in heavy-loaded lines might be increased under traditional security constraints. Meanwhile, the power generation and dispatch schemes have been readjusted to adapt to the market clearing in China because of its infancy reform since 2015 [2][3], which aggravates the issue. Therefore, an improved clearing model is required to confront such challenges.

However, electricity power market clearing models still experience shortfalls in light of network congestion [4][5]. A relatively conservative dispatch margin was reserved in network constraints to ensure the safe operation of the power system generally, which leads to the low line utilization rate. Two main reasons cause the problem. Firstly, existing mainstream clearing models are solved based on DC optimal power flow (DCOPF). Thus, the calculated power flow deviation between the clearing results and real conditions is difficult to be eliminated for imprecision in the DC power flow model compared with the AC power flow model [6], where the deviation will be named as 'AC/DC deviation' in the following. Power flow congestion might be misjudged with the increasing load when some line is heavy-loaded. Secondly, static line rating (SLR), used to determine the maximum transmission capacity, will lead to a lower line utilization rate due to underestimation of the available line rating in various weather conditions [7].

Moreover, real-time market (RTM) demands accurate market clearing results in the shortest time periods. The contradictory requirements between accuracy and expeditiousness are hard to be obtained. These characteristics also make the heat balance equation (HBE) for dynamic line rating more difficult to be integrated into existing real-time market clearing models. Thus, real-time conductor temperature is impossible to be calculated dynamically.

Several researches have been conducted on reducing AC/DC deviation [8]-[13]. On one hand, network loss has been improved. Reference [8]-[12] discussed the network loss approximation and its transmission. However, losses cannot be calculated precisely in the linear clearing model due to the squared term of current. On the other hand, the power flow

This work was supported by HUST-State Grid Future of Grid Institute (521209200014). (*Corresponding author: Xinyu Chen*.)

Hongyu Pan, Xinyu Chen, Tianyu Jin, and Jinyu Wen are with the State Key Laboratory of Advance Electromagnetic Engineering and Technology, Huazhong University of Science and Technology, Wuhan 430073, China (e-mail: hy_pan99@hust.edu.cn; xchen@seas.harvard.edu; ty_jin@hust.edu.cn; jinyu.wen@hust.edu.cn)

Yang Bai and Zhongfei Chen are with Guangdong Power Grid Co., Ltd Power Dispatch and Control Center Guangdong, China (e-mail: baiyang@gddd.csg.cn; 524324960@qq.com)

Qiuwei Wu is with the Center for Electric Power and Energy, Department of Electrical Engineering, Technical University of Denmark, 2800 Kgs. Lyngby, Denmark (e-mail: quiwudtu@gmail.com).

model has been improved. Reference [13] proposed a linearized optimal power flow model with reactive power and voltage magnitude based on Taylor expansion. However, such studies cannot be applied into existing RTM clearing models solved by linear programming due to the nonlinear terms of voltage and phase angle. Meanwhile, the active and reactive power balance demands massive calculations with a longer time, which cannot adapt to the short time periods in RTM. Moreover, no existing researches consider the essence of power flow distribution and propose innovations from the perspective of power transfer distribution factor (PTDF) correction. Thus, the AC/DC deviation cannot be reduced fundamentally.

Several researches have also been carried out on the calculation of dynamic line rating (DLR) in optimal power flow under the transmission system [14]-[24]. Reference [15]-[17] proposed the calculation methods of DLR. However, these studies cannot calculate the real-time conductor temperature efficiently and fast in DCOPF because of many nonlinear terms in steady-state heat balance or complicated models. Reference [18]-[24] applied DLR calculation into AC optimal power flow problems in the day-ahead operation and real-time market of the power system. However, such studies demand massive calculations with a long time on the active and reactive power balance, which is hard to adapt to the short time periods in RTM.

This paper proposes an improved real-time market clearing model considering PTDF correction and fast-calculated dynamic line rating. PTDF correction based on Taylor expansion approximation improves the accuracy of power flow distribution. Improved dynamic line rating model with faster speed in calculating real-time conductor temperature further reduces the relatively conservative dispatch margin. Moreover, the line utilization rate can be improved due to elastic network constraints according to various weather conditions. In the context of the previous research, our paper provides the following contributions.

1) We propose an improved real-time market clearing model using DCOPF based on PTDF correction to reduce the AC/DC deviation. The correction factor is first derived from the AC power flow by Taylor expansion, then simplified by combining the characteristic such as the short time periods in RTM. The proposed model avoids the extensive computation of active and reactive power balances and improves the calculation accuracy of the DC power flow model without increasing the amount of calculation, which is also convenient to be integrated into the existing RTM model based on DCOPF.
2) We propose a fast-calculated dynamic line rating model in DCOPF based on the piecewise linear approximation method. The model considers the weather condition changes across the line spans and is simplified from the most rigorous dynamic line rating model at the dispatch level. During each time period, HBE can be represented by linear expressions at the dispatch level. The maximum transmission capacity can be adjusted flexibly according to ambient temperature and weather conditions.
3) We test and verify the validity of the proposed model in three independent systems, which are the IEEE 39-bus system, IEEE 2383-system, and the real power grid in Yunnan province of China, respectively. The results have been proven effective in the real-world electricity spot market, which provides a reference for power grid system or electricity spot market in similar situations.

The structure of the paper is the following: Section II presents PTDF correction derivations based on an improved power flow model via Taylor expansion approximation. Section III presents the piecewise linear approximation method to calculate real-time conductor temperature, and formulates the improved real-time market clearing model considering fast-calculated dynamic line rating. Three independent systems simulation results of the proposed model, as well as analysis of four different methods, are presented in Section IV. Conclusions are presented in Section V.

We note that a preliminary conference paper addressed the issue of AC/DC deviation in [25], and this paper extends the more refined correction derivations and improved dynamic line rating model. The clearing model with network constraints representation and the iteration algorithm in RTM has also been researched further.

## II. PTDF CORRECTION DERIVATIONS

Here, we formulate the improved clearing model by PTDF correction. The mathematical model is derived from the improved power flow model in RTM based on Taylor's expansion with voltage and angle approximation combing with the real-time market characteristics. Quasi-steady-state correction is also considered to increase stability. We also improve the method to calculate marginal line losses more accurately.

### *A. Improved Power Flow Model in RTM*

Using the AC power flow model and ignoring the transformers, power flow through branch $k \in K$ can be defined from node *i* to *j*,

$$P_{ijk} = g_{ijk}(v_i^2 - v_i v_j \cos\theta_{ijk}) - b_{ijk} v_i v_j \sin\theta_{ijk} \tag{1}$$

where $g_{ijk}$ and $b_{ijk}$ represent the branch conductance and susceptance respectively.$\theta_i$ is the phase angle and $v_i$ represents the voltage magnitude. Formula (1) is applicable to the case of a single line with two nodes connected. Parallel processing is necessary when multiple lines are connected.

In actual power system operation, the fluctuation of phase angle and voltage is relatively small. Therefore, three main assumptions have been proposed on the simplified AC power flow approximation:

(i) Voltage multiplied with angle is close to one per unit (p.u.) at all nodes, which means $v_i v_j \theta_{ij} \approx \theta_{ij}$.

(ii) Voltage multiplied with branch conductance can be rewritten to another form, which means,

$$\frac{1}{2} g_{ijk} v_{ij}^2 \approx \frac{1}{2} g_{ijk} \left(\frac{v_i + v_j}{v_{i,0} + v_{j,0}}\right)^2 v_{ij}^2 \tag{2}$$

(iii) Phase angle differences are small, i.e.,

$$\sin\theta_{ij} \approx \theta_{ij}, \cos\theta_{ij} \approx 1 - \frac{1}{2}\theta_{ij}^2 \tag{3}$$

Furthermore, the Taylor expansion of voltage and phase angle is carried out as follows:

$$\frac{1}{2}g_{ij}\theta_{ij}^2 \approx g_{ij}\theta_{ij,0}\theta_{ij} - \frac{1}{2}g_{ij}\theta_{ij,0}^2 \tag{4}$$

$$\frac{1}{2}g_{ij}\left(\frac{v_i+v_j}{v_{i,0}+v_{j,0}}\right)^2 v_{ij}^2 \approx g_{ij}\frac{v_{i,0}-v_{j,0}}{v_{i,0}+v_{j,0}}(v_i^2-v_j^2) - \frac{1}{2}g_{ij}(v_{i,0}-v_{j,0})^2 \tag{5}$$

Here, we use the initial or the last moment state for the base conditions to fit the voltage $v_{i,0}$, $v_{j,0}$ and phase angle $\theta_{ij,0}$.

Combining equations from (1) to (5) formulates the simplified AC power flow model,

$$P_{ij} = g_{ij}\left(1+2\frac{v_{i,0}-v_{j,0}}{v_{i,0}+v_{j,0}}\right)\left(\frac{v_i^2-v_j^2}{2}\right) + (g_{ij}\theta_{ij,0}-b_{ij})\theta_{ij} - \frac{1}{2}g_{ij}[\theta_{ij,0}^2+(v_{i,0}-v_{j,0})^2] \tag{6}$$

where $v_{i,0}$, $v_{j,0}$ are the voltages and $\theta_{i,0}$, $\theta_{j,0}$ are the phase angles in base condition.

Equation (6) is more accurate compared with the traditional DC power flow model. However, voltage is still in a high power state, which cannot be integrated into linear programming in security constrained economic dispatch (SCED). In real-time market, the load fluctuation is generally small between time periods, as well as the voltage amplitude and phase angle fluctuations. So we choose the forecasting solution or the day-ahead market results to replace the voltage variable and simplify the phase angle terms by considering the characteristics. The approximation can be represented as,

$$(g_{ij}\theta_{ij,0}-b_{ij})\theta_{ij} \approx -b_{ij}\theta_{ij} \tag{7}$$

$$v_i \approx v_{i,0}, v_j \approx v_{j,0} \tag{8}$$

Finally, the improved power flow model in real-time market can be expressed by,

$$P_{ij} = -b_{ij}\theta_{ij} + g_{ij}\left(1+2\frac{v_{i,0}-v_{j,0}}{v_{i,0}+v_{j,0}}\right)\left(\frac{v_{i,0}^2-v_{j,0}^2}{2}\right) - \frac{1}{2}g_{ij}[\theta_{ij,0}^2+(v_{i,0}-v_{j,0})^2] \tag{9}$$

Equation (9) has two parts. The first part is the traditional DC flow model formulated as $-b_{ij}\theta_{ij}$, and the second part can be regarded as a constant decided by the real-time grid state. For convenience, we name the second part the Taylor factor $T_{ij}$.

### *B. PTDF correction*

PTDF is the core of DCOPF defined as the ratio of the power flow distribution on each line to the total power flow injected into the network, which is derived from the traditional DC power flow model [26],

$$P_s = B\theta_s \tag{10}$$

$$P_s = M_{m,n}\cdot\omega \tag{11}$$

where $P_s$ is the vector of node real power injections, $B$ is the node susceptance matrix, $\theta_S$ is the vector of node phase angles, $M_{m,n}$ is the node-transaction incidence vector, and $\omega$ is the value of transactions from node $m$ to node $n$.

Combing (10) and (11) gives,

$$\theta_s = B^{-1}\cdot M_{m,n}\cdot\omega \tag{12}$$

Each branch power flow can be calculated by the difference of phase angles, which means,

$$P_{mn} = -b_{mn}M_l^T\theta_s \tag{13}$$

where $M_l^T$ is the node-branch incidence vector.

Combing (12) with (13), the traditional PTDF on branch $l$ from node $m$ to $n$ is,

$$PTDF_{m,n,l} = \frac{1}{x_l}M_l^T B^{-1} M_{m,n} \tag{14}$$

where $x_l$ is the reactance on branch $l$.

Replacing equation (13) by (9), then the PTDF correction on branch $l$ is given,

$$PTDF_{m,n,l}^C = PTDF_{m,n,l} + k\cdot C_l \tag{15}$$

where $k$ is the scale factor, $C_l$ is the PTDF correction factor defined as $T_l/P_l$, $T_l$ is the Taylor factor on branch $l$, and $P_l$ is the power flow on branch $l$. The sign of $C_l$ is related to the direction of the line flow, which is positive when the flow is in the same direction as the given positive direction, and negative when opposite.

Equation (15) is applicable to a single power flow injection. In the actual power grid, multiple power flows are injected into the network simultaneously. In this case, we further extend the model to the matrix form,

$$\Psi = \begin{bmatrix} \psi_1^{w_1} & \psi_1^{w_2} & \cdots & \psi_1^{w_N} \\ \psi_2^{w_1} & \psi_2^{w_2} & \cdots & \psi_2^{w_N} \\ \vdots & & \ddots & \\ \psi_L^{w_1} & & & \psi_L^{w_N} \end{bmatrix} \tag{16}$$

where $\psi_l^w$ is the ratio of power flow in the $l$-th line to the $w$-th transaction injecting to the grid. Equation (16) represents the case with $n$ power flows and $l$ transactions in any network, and the corresponding PTDF can be calculated as follows,

$$\Psi = x_b^{-1}\begin{pmatrix} M_1^T \\ M_2^T \\ \vdots \\ M_L^T \end{pmatrix} B^{-1}\begin{pmatrix} M_{w_1} & M_{w_2} & \cdots & M_{w_N} \end{pmatrix} + C \tag{17}$$

where $x_b$ is the reactance matrix, and $\boldsymbol{C}$ is the correction factor matrix.

Quasi-steady-state sensitivity correction is also considered to overcome the shortcoming that traditional PTDF analysis cannot simulate the physical response of the actual power system [27],

$$PTDF^{CQ} = PTDF^C\cdot F_u \tag{18}$$

where $F_u$ is the linearized coefficient matrix expressing the quasi-steady-state physical response of the control variable to system disturbance.

In the electricity market, $F_u$ can generally be calculated as,

$$F_u = I - \alpha \cdot 1^T \tag{19}$$

where $\alpha$ is the active power distribution factor determined by the output of each node usually, $I$ is a unit matrix, and **1** is a vector in which all the elements are 1.

### C. Marginal Line Losses Correction

Marginal line losses is a method to calculate the network losses without the square terms, which is reflected on each node through the loss distribution factor. Based on the above assumptions, the line losses is given as a multiplication of line resistance $r_l$ and quadratic function of power flow $P_l$,

$$loss = \sum_l r_l P_l^2 \tag{20}$$

In the improved power flow model approximation, nodal injections are related to real power flow by PTDF. The power flow $P_l$ is determined as,

$$P_l = \sum_n PTDF_{n-l}^{CQ} \times P_n \tag{21}$$

where $P_n$ is the net load of the $n$-th node.

The loss factor defines the linear sensitivity of total system losses to real power injections in each node. Equation (21) leads to the following calculation for loss factor,

$$LF_n = 2\sum_l r_l \cdot \bar{P}_l \times PTDF_{n-l}^{CQ} \tag{22}$$

The system marginal line losses can be given as,

$$loss = loss_0 + LF^T \left( P_g - P_d \right) \tag{23}$$

where $loss_0$ is a constant calculated at the base point, $P_g$ is the unit output vector and $P_d$ is the demand vector.

## III. Real-Time Market Clearing Model

Here, the piecewise linear approximation method is proposed to adapt to the characteristics of short time periods in RTM. The step current assumption is also presented to simplify the calculation. Then an iterative clearing algorithm and the real-time market clearing model with improved network constraints representation considering PTDF correction and DLR will be introduced.

### A. DLR in Real-Time Market

The safe and stable operation of the power grid is crucial in real-time market, which not only considers the maximum transmission capacity constraints, but also pays attention to whether the conductor temperature would cause potential thermal problems due to various weather conditions or peak load. The conductor temperature depends on 1) ambient temperature and weather conditions, 2) line current, and 3) conductor physical parameters, and the representative formula is the heat balance equation [28]. The HBE is composed of heat gain and heat loss. The heat gain consists of solar heat gain and Joule heat gain, while the heat loss is convective heat loss and radiated heat loss terms. It reflects the heat energy that enters, leaves and gets stored in the conductor per unit time, causing the temperature change [29]. Two types of HBE are derived, one is applied to the 'Steady-state heat balance',

$$q_c + q_r = q_s + q_j \tag{24}$$

and the other is applied to the 'Non-steady-state heat balance',

$$q_c + q_r + m \cdot C_p \cdot \frac{dT_s}{dt} = q_s + q_j \tag{25}$$

where $q_c$ and $q_r$ represent the convective and radiated heat loss rates respectively, the solar heat gain rate is expressed as $q_s$ and $q_j$ is the Joule heating, which can also be represented by line losses. $T_s$ is the conductor surface temperature, restricted by the maximum allowable temperature in the power system operation, $mC_p$ represents the total heat capacity of the conductor and $dT_s/dt$ represents the time derivative of the conductor temperature.

Assuming that the steady-state current and temperature are given, when the current step occurs, it takes almost one hour for the conductor temperature to reach a new steady-state thermal balance with the 1-minute calculation interval. The temperature changes rapidly in the first tens of minutes, and climbs gradually during most of the remaining time. Therefore, in the entire period, the conductor temperature has the linear characteristic in the first ten minutes, which coincides with the short time periods in RTM.

In addition, DLR is highly dependent on weather conditions. The span lengths of conductors and corresponding ambient weather changes in DLR systems will affect the actual temperature of the conductors. The real-time status of the conductor needs to be dynamically monitored, including the adverse sagging, the wire tension and the angle of the wire cut by the wind in different weather. These accurate models will be critical to efficiently compute the dynamic line rating and provide reliable load ability information.

However, the real-time dispatch model, due to the limitation of short scheduling periods and complex calculations in the dispatch center of parameters such as sagging, the line tension and the line section angle, has to be simplified from the most rigorous dynamic line rating model. The dispatching center only needs to calculate the power flow of the system according to the transmission data to allocate the output of the unit. Therefore, we have conducted our study at the dispatch level and simplified the calculation of corresponding data in our model for practical engineering considerations in DCOPF. One real-time market time period is 15 minutes. Load data, bidding prices and weather conditions are provided to the dispatching center every time period. During the 15 minutes, the dispatch center will adjust network constraints based on the conductor temperature, which is calculated by the weather conditions across the line spans in each monitoring region and the expected current value. Starting from the initial state of the time period, the conductor temperature is calculated every minute. Then the conductor convection and radiant heat loss items are updated according to the calculated temperature every minute, while the solar energy and Joule heating gain remain unchanged. The temperature at the end of the time period will be obtained after iterating 15 times in this way.

According to the results, the conductor temperature presents an approximately linear trend within one time period in RTM. So the piecewise linear approximation method for the conductor temperature can solve the above problems. The

**Algorithm: Improved Real-Time Market Clearing**

**Input:** Voltage $V_t$, phase angle $\theta_t$, load $P_t^D$, bidding price $B_t$, and other basic parameters in the scheduling time period.

**Output:** Unit outputs $P_t^G$ and market clearing price at the corresponding period.

**For** all $t \in \tau$

Obtain the parameters such as voltage, phase angle, marginal line losses and power flow at the base time period.

**do**

**i)** Solve real-time market clearing based on the improved model in (29).

**ii)** Solve the actual power flow of the clearing results using AC Newton-Raphson's method and calculate AC/DC deviation.

**iii)** Check SLR and DLR lines overload information.

**If** Power or thermal overload lines exist.

Update the parameters such as voltage, phase angle, marginal line losses and power flow at the new condition. Correct PTDF and network constraints of the model in (29d) and (29e).

**Else**

End the iteration.

**End**

**While** System actual security requirements are met.

The unit outputs and market clearing prices are given.

**End**

Fig. 1. Algorithm of the improved real-time market clearing model.

conductor temperature at the end of the time period can be expressed as,

$$T_{15} = T_0 + \left( \sum_{i=1}^{U} c_i l_i K \right) \cdot 15 \tag{26}$$

$$\sum_{i=1}^{U} c_i = 1 \tag{27}$$

where $T_0$ is the conductor temperature at the initial moment, $T_{15}$ is the conductor temperature in the 15-th minute, $U$ is the number of segments divided by one time period, $c$ is the coefficient corresponding to each segment, $l$ is the length of each segment and $K$ is the tangent of the temperature curve at the initial moment. It can be obtained by deriving the temperature function, or calculated by a physical expression:

$$K = \frac{\left( q_{j,0} + q_{s,0} - q_{c,0} - q_{r,0} \right)}{m \cdot C_P \left( T_{s,0} - T_{a,0} \right)} \tag{28}$$

where $T_{a,0}$ is the ambient temperature at the initial moment. At the initial moment of each time period, parameters in (28) can be obtained through device observation. So $K$ can be calculated before scheduling. By linearizing the HBE, we can calculate the temperature at the end of the time period.

In addition, the age and loading induced failure of the lines with aleatory uncertainty and epistemic uncertainty, which is illustrated by the Arrhenius and Weibull models, are needed to be considered when our model is used in the power grid for a long time [30][31]. The failure rate of the existing lines should be calculated in RTM and the proportion of DLR applied in the system should be adjusted according to the desired expected-energy-not-served (EENS) value.

The accuracy of our model will also be affected by the cyber layer when a signal transmission interruption occurs. In order to address the issues, the cyber layer can be established to interface with the existing physical layer via phasor measurement units (PMU) deployment across the network, providing monitoring and protection functions for DLR and system integrity protection schemes (SIPS) implementation [32][33]. When weather data uncertainty occurs, the use of fuzzy sets in DTR calculations, known as Fuzzy-DTR-OTS (FDTR-OTS), is also an effective method to enhance network reliability [34].

### *B. Improved Real-Time Market Clearing Model*

The real-time market clearing model is summarized as follows:

$$\min \sum_{t=1}^{\tau} \sum_{j=1}^{J} B_{j,t} \left( P_{j,t}^G \right) \tag{29a}$$

$$\text{s.t.} \quad P_t^G - P_t^D = loss_t, \qquad \forall t \tag{29b}$$

$$loss_t = loss_{t,0} + LF^T \times \left( P_t^G - P_t^D \right), \qquad \forall t \tag{29c}$$

$$PTDF^{CQ} \times \left( P_t^G - P_t^D - LD \cdot loss_t \right) + Pf_t^+ \le P_k^{\max}, \ \forall k \in \mathrm{Z}, \forall t \tag{29d}$$

$$PTDF^{CQ} \times \left( P_t^G - P_t^D - LD \cdot loss_t \right) + Pf_t^- \le -P_k^{\max}, \ \forall k \in \mathrm{Z}, \forall t \tag{29e}$$

$$T_{k,s,t} \le T_t^{\max} \qquad \forall k \in \mathrm{Z}, \forall s \in S, \forall t \tag{29f}$$

$$P_{j,t}^{G\min} \le P_{j,t}^G \le P_{j,t}^{G\max}, \qquad \forall j, \forall t \tag{29g}$$

$$-\Delta P_j^{GD} \le P_{j,t}^G - P_{j,t-1}^G \le \Delta P_j^{GU}, \qquad \forall j, \forall t \tag{29h}$$

$$\Delta SR_t^U \le \sum_{j=1}^{J} P_{j,i+1}^{G\max} - P_{j,t} \le -\Delta SR_t^D, \qquad \forall j, \forall t \tag{29i}$$

The cost objective function is minimized as (29a), in which $B_j(\cdot)$ is the bidding price function of unit $j$ and $P_{j,t}^G$ is the output of unit $j$ in time period $t$. $j \in J$ is the index and set of units, and $t \in \tau$ is the index and set of time periods. Load balance is established by (29b), and marginal line losses is calculated by (29c), in which $P_t^G$ and $P_t^D$ are the unit output vector and load demand vector in nodes respectively. The power flow are constrained by (29d) and (29e), where $k \in \mathrm{Z}$ is the index and set of network lines. $PTDF^{CQ}$ is the PTDF correction matrix of the grid, and $LD$ is the vector of loss distribution factors. $Pf^+$, $Pf^-$ are the dynamic line constraints for positive and negative trends, respectively, and $P_k^{max}$ is the maximum transmission capacity of the $k$-th line. $s \in S$ is the index and set of regions. The

TABLE I
DEFINITION OF THE FOUR METHODS

| Method | Definition |
|---|---|
| SLR | traditional DCOPF method with static line rating |
| SLR-L | DCOPF method considering marginal line losses with static line rating |
| SLR-C | DCOPF method considering PTDF correction, marginal line losses and iteration with static line rating |
| DLR-C | DCOPF method considering PTDF correction, marginal line losses and iteration with dynamic line rating |

maximum allowable conductor temperature limits at time period $t$ are given by (29f), which is determined by the worst weather conditions across the conductor span. Active power limits are imposed by (29g), where $P_{j,t}^{Gmin}$, $P_{j,t}^{Gmax}$ are the minimum and maximum output of unit $j$ in time period $t$. Unit output are constrained by ramp-up rates as well as by ramp-down rates (29h), where $\Delta P_i^{GU}$, $\Delta P_i^{GD}$ are the ramp-up limit and ramp-down limit of the unit $j$. Equation (29i) gives the spinning reserve constraints, in which $\Delta SR_t^U$, $\Delta SR_t^D$ are the spinning-up reserve requirement and spinning-down reserve requirement in time period $t$.

Based on the theory derived from Section II, SCED for power systems can be implemented by the improved real-time market clearing method as illustrated in Fig.1. The parameters will be updated and iterated during the whole clearing process in real time until the system actual security requirements calculated by AC method are met. In the initial operation, the amount of calculation will be relatively large. In subsequent operations, the calculation time will be reduced due to the little difference between the parameters of adjacent time periods.

Compared with existing clearing models, the network constraints in our model are improved by (29d)-(29f) during the iteration to increase the line utilization rate. PTDF correction increases the accuracy of clearing results through the improved power flow model in RTM, and fast-calculated dynamic line rating adjusts the maximum transmission capacity flexibly according to various weather conditions. $Pf^+$, $Pf^-$ are also applied into clearing to further reduce the AC/DC deviation.

## IV. CASE STUDY

The proposed method has been implemented in three different independent systems, which are the IEEE 39-bus system, the IEEE 2383-bus system and the real-world power system in Yunnan province of China. Four methods are compared to illustrate the gap between the models, which are SLR, SLR-L, SLR-C and DLR-C shown in TABLE I. To evaluate the effectiveness of the proposed method, this section is divided into two parts. The first section tests the improvement in reducing AC/DC deviation using PTDF correction. The second section shows the further impact and promotion of SLR-C using dynamic line rating.

### A. Test of PTDF correction

Three independent systems are used to illustrate the effect of reducing AC/DC deviation, and curves all refer to the real daily operation of Yunnan province in China on a typical day. The cases are chosen as follows:

Case I: IEEE 39-bus system with actual data in Yunnan

Case II: IEEE 2383-bus system with actual data in Yunnan

Case III: the real power system in Yunnan province of China

The 39-bus system consists of 39 nodes and 46 branches, among which the thermal generators are set up at 30~39 nodes with reference node 31. The IEEE 2383-bus system has 2383 nodes and 2896 lines. Compared to Case I, this system has more complete node line mapping similar to the real-world system, which contains multi-energy power generators. The real power grid system in Yunnan province contains 1691 nodes, 2149 lines or sections and 387 multi-energy power generators including large-scale cascade hydropower stations, runoff hydroelectric power stations, thermal power, wind power and photovoltaics.

We calculate real-time market clearing at 96 time periods in a single day based on model predictive control in given network constraints, and then make corresponding comparisons for the AC/DC deviation and line utilization rate. Two time dimensions are analyzed to compare the four methods, which are the single time period and total time period, respectively.

*1) Single time period:* We choose a typical time period in 96 time periods for the AC/DC deviation analysis, which is the peak load time period in the 68-th point. In the period, AC/DC deviation comparison in branches has been illustrated in Fig. 2.

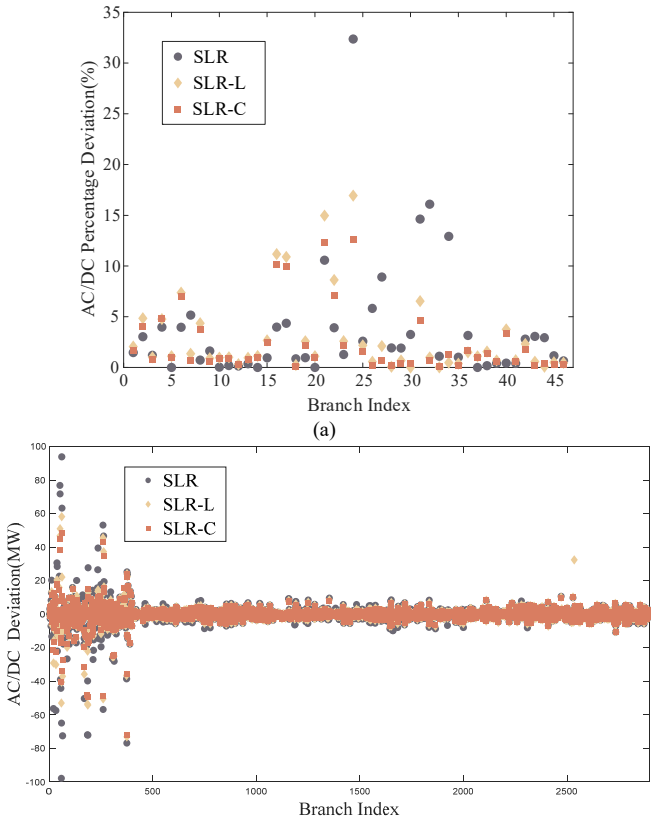


Fig. 2. AC/DC deviation comparison in peak time period among SLR, SLR-L and SLR-C. (a) AC/DC percentage deviation in Case I; (b) AC/DC deviation in Case II.

TABLE II
PARAMETERS OF THE PEAK TIME PERIOD IN IEEE CASE SYSTEMS

| Case | Method | Variance (MW) | Maximum Deviation (MW) | Total Deviation (MW) |
|---|---|---|---|---|
| I | SLR | 503.68 | 100.93 | 531.52 |
| | SLR-L | 17.02 | 14.81 | 273.58 |
| | SLR-C | 11.33 | 11.25 | 227.45 |
| II | SLR | 36.790 | 97.800 | 6352.3 |
| | SLR-L | 18.170 | 73.076 | 5171.7 |
| | SLR-C | 14.844 | 71.884 | 4901.9 |

TABLE III
RELATIVE AC/DC DEVIATION (%) IN TYPICAL LINES OF THE WHOLE DAY IN YUNNAN PROVINCE

| Case | Line Name | SLR | SLR-L | SLR-C |
|---|---|---|---|---|
| III | The BaoJiu II line | 6.8053 | 4.7591 | 3.9477 |
| | The Duohong III line | 17.4400 | 13.1393 | 10.0995 |
| | The Tongda III line | 16.0383 | 14.8433 | 13.0608 |
| | The Wenkai I line | 8.9912 | 8.1353 | 7.8487 |
| | The Daxia I line | 7.1547 | 5.6480 | 5.0410 |

In most of lines, the deviations of SLR-L and SLR-C have been reduced to varying degrees compared to SLR while some increased for the power flow redistribution. SLR-L performs better than SLR generally. Among them, SLR-C is the most accurate method.

In addition, the variance, maximum AC/DC deviation and total AC/DC deviation of lines decrease in turn by comparing the three methods. In Case I, the variances are 503.68, 17.02 and 11.33, the maximum AC/DC deviations are 100.93MW, 14.81MW and 11.25MW, and the total deviations are 531.52MW, 273.58MW and 227.45MW, corresponding to SLR, SLR-L and SLR-C, respectively. In Case II, the variances are 36.790, 18.170 and 14.844, the maximum AC/DC deviations are 97.800MW, 73.076MW and 71.884MW, and the total deviations are 6352.3MW, 5171.7MW and 4901.9MW, corresponding to SLR, SLR-L and SLR-C, respectively. By contrast, SLR is the worst, SLR-L is relatively better, and SLR-C is the best. The detailed data is shown in TABLE II.

*2) Total time period:* Apart from the peak load time period, the operation of the whole day is also worthy of attention. Thus, we further analyze AC/DC deviation throughout 96 time periods. The AC/DC deviation of each time period is added by the AC/DC deviation in each branch at the time period, and all parameters are the sum of clearing data of 96 time periods.

We analyze the total AC/DC deviation among SLR, SLR-L and SLR-C. As shown in Fig. 3, the deviation and the load curve have roughly the same trend, with a smaller value at valley load and a larger value at peak load. In Case I, the deviation of the whole day in SLR is relatively large, with a total value of 41942.37MW, accounting for 5% of the daily output. SLR-L makes up for the inaccuracy of DCOPF, optimizes the scheduling results, and reduces the overall AC/DC deviation to 21657.78MW. On this basis, SLR-C further reduces the AC/DC deviation to 17545.53MW. In the total time period, the AC/DC deviation in SLR is relatively large, with a total value of 503526.1776MW. SLR-L reduces the overall AC/DC deviation

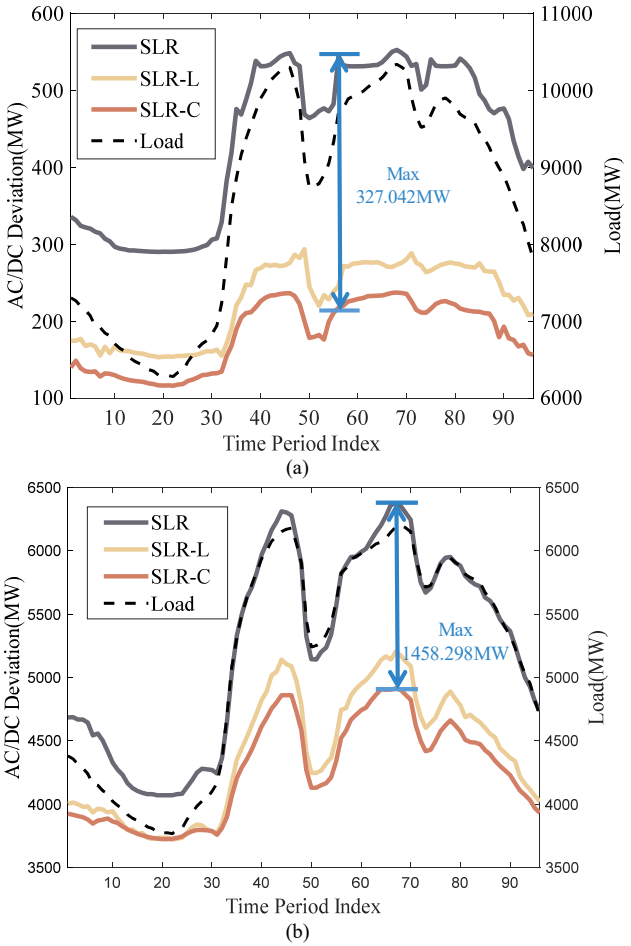


Fig. 3. Total AC/DC deviation of the daily operation among SLR, SLR-L and SLR-C. (a) Parameters in Case I; (b) Parameters in Case II.

to 422430.3812MW. On this basis, SLR-C further reduces the AC/DC deviation to 413260.5167MW, where the scheduling accuracy of the whole day is improved by about 2% compared to SLR-L. In Case II, the AC/DC deviation in SLR is 503526.1776MW. SLR-L reduces the overall AC/DC deviation to 422430.3812MW. SLR-C further reduces the AC/DC deviation to 413260.5167MW, where the scheduling accuracy of the whole day is also improved by about 2% compared to SLR-L. The detailed data is shown in Fig. 3. Therefore, in the daily dimension, SLR-C is still the best choice with an average 2% promotion in SLR-L.

Furthermore, we have conducted the simulation in the real-world electricity power market environment in Yunnan province. The load data, the wind and the photovoltaic output of a typical day from the actual power system in Yunnan are employed to justify the effectiveness. Considering that its actual power flow needs to be kept confidential, here we will show the statistical data in the typical lines.

The Baojiu II line, the Duohong III line, the Tongda III line, the Wenkai I line and the Daxia I line are used for analysis, which carry important transmission tasks and often cause network congestion. The data are shown in TABLE III in detail. The results show that the relative deviations of SLR-L and SLR-C have been significantly reduced compared to SLR in the five typical lines. SLR-L performs better than SLR generally

This article has been accepted for publication in IEEE Transactions on Industry Applications. This is the author's version which has not been fully edited and content may change prior to final publication. Citation information: DOI 10.1109/TIA.2022.3218271





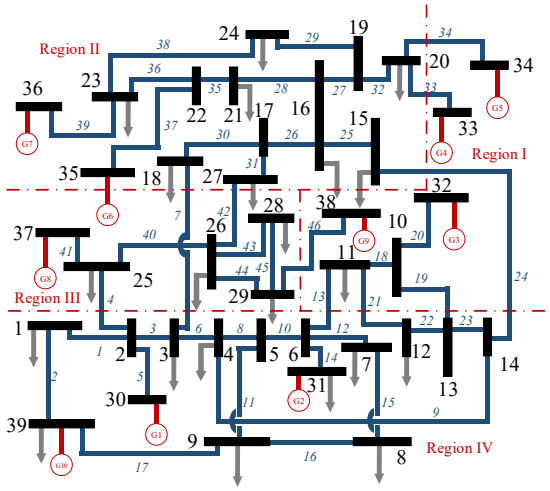


Fig. 4. Power grid topology of the 39-bus system.

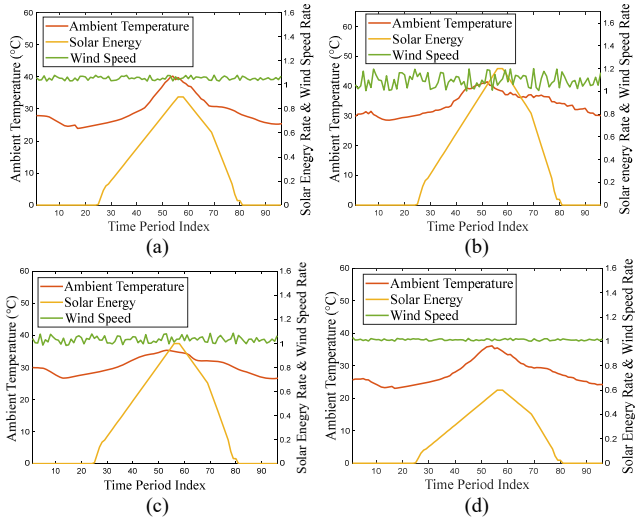


Fig. 5. Ambient temperature and weather conditions. (a) Parameters in Region I; (b) Parameters in Region II; (c) Parameters in Region III; (d) Parameters in Region IV.

with an average of 3% promotion. SLR-C further reduces the relative AC/DC deviation with an average of 2% improvement. The SLR-C solution performs best on The Duohong III line, where the relative AC/DC deviation is reduced by 7.3% lower than that of the traditional DCOPF. SLR-C can effectively reduce the dispatch margin of these lines due to congestion, thereby improving grid security, which is the most accurate method in the actual real-time electricity market operation of Yunnan province.

### *B. Impact of dynamic line rating based on SLR-C*

Here the 39-bus system is used for simulation. It is further geographically divided into four areas (Region I-IV) and then sectionalized with respect to different stations, which is shown in Fig. 4. The monitoring stations for weather conditions have been set in each area and transmit data continuously to the dispatching center in real time. The data transmitted to the dispatch center is assumed to be the actual value.

Assuming that the system is stable at 0:00, the calculation interval of the heat balance equation is selected as 1 minute. The temperature is measured every 15 minutes as one period in real-time market. The ambient temperature and weather conditions in each region are shown in Fig. 5. The ambient temperature fluctuates around 30℃, which is low in the morning and evening, while high at noon. Solar energy starts to rise at about 6 am, reaches its peak at about 1 pm, and then decreases until disappears at about 8 pm. The wind speed rate fluctuates randomly with a reference of 0.61m/s perpendicular to the conductor. Al-St hinged conductor is used for analysis, and the maximum allowable conductor temperature of this material wire is 100 degrees Celsius.

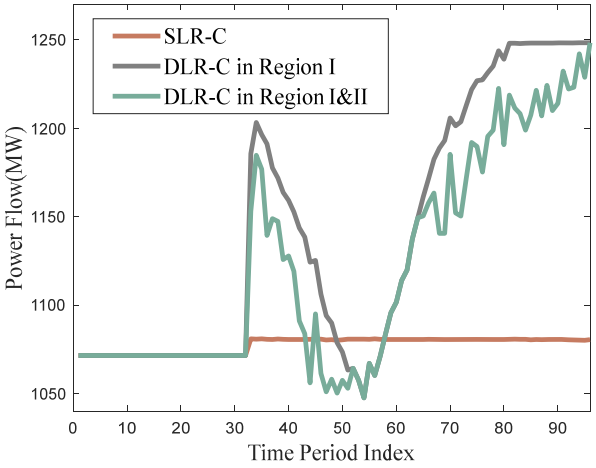


Fig. 6. Power flow in the 33-rd line between SLR-C and DLR-C.

The 33-rd line is one of the most important transmission lines, which spans Region I and Region II. Hence, its DLR will be determined by the worst weather conditions in the two areas. We conducted a comparison of the power flow in the 33-rd line between the two cases. The first is to ignore the line spans and their surrounding weather conditions, and the system is only in the weather conditions shown in Region I. The second takes into account line spans and surrounding weather changes, where the system is geographically divided into four regions and the 33-rd line passes through Region I&II. The result shows that the power flow in the 33-rd line reduced after considering the conductor span and weather conditions, as shown in Fig. 6.

Meanwhile, we analyze the relatively conservative dispatch margin reserved. We illustrate the issue by comparison of power flow changes in the 33-rd line between SLR-C and DLR-C. The 33-rd line is selected because its power flow is the largest, creating the most Joule heating. During peak load periods at noon and evening, the conductor temperature reaches the highest point. In SLR-C, under the given network constraints of the power grid and weather conditions, the temperature variation of the third branch is calculated iteratively by HBE. The maximum transmission capacity of the 33-rd line is formulated according to the critical temperature limit. Therefore, its power flow constraint can only be limited to about 1080MW throughout the day, even if the temperature decreases at night. When we introduce DLR into real-time market through the piecewise linear approximation method, the power flow has been greatly improved. As the temperature decreases, the power flow gradually increases, and finally reaches about 1250MW, making full use of the maximum

TABLE IV
COMPARISONS OF LINE AVERAGE UTILIZATION RATE

| Line Average Utilization Rate (%) | Maximum Transmission Capacity (MW) | SLR | SLR-L | SLR-C | DLR-C |
|---|---|---|---|---|---|
| 5-th | 1100 | 75.781 | 77.393 | 77.595 | 78.052 |
| 14-th | 900 | 86.715 | 88.307 | 88.684 | 89.622 |
| 33-rd | 1250 | 79.407 | 83.371 | 86.133 | 89.946 |
| 46-th | 1000 | 84.449 | 85.810 | 86.239 | 90.073 |

transmission capacity, which is also illustrated in Fig. 6. In addition, the results indicate that power flow increments presented in Fig. 6 may not be positive in some rare cases for the consideration of gird security. At these moments, due to the harsh weather condition, the dynamic line rating is in fact lower than its static line rating value.

We further select four lines with heavier power flow and higher conductor temperature in the system to analyze the line utilization rate, which are the 5-th, the 14-th, the 33-rd and the 46-th lines, respectively. We calculated the line average utilization rate of 96 points in the four methods and the detailed data is shown in TABLE IV. The data proves that the line average utilization rate increases gradually in four methods. SLR is the lowest and SLR-L is better with about 2% promotion. Compared with SLR-L, SLR-C improves the line average utilization rate with 0.2~3% promotion. DLR-C further increases the line utilization rate by dynamic line rating based on SLR-C with an average of 2.3% promotion, which is the highest among all methods.

## V. CONCLUSION

In this paper, a real-time power market clearing model with improved network constraints considering PTDF correction and fast-calculated DLR is proposed. The PTDF correction derived from the improved power flow model in RTM is proposed first. The mathematical model is formulated based on Taylor expansion with voltage and phase angle approximation from the AC power flow model. Quasi-steady-state correction and marginal line losses correction are applied into the clearing model further. Meanwhile, dynamic line rating has been integrated into RTM by piecewise linear approximation method to calculate real-time conductor temperature faster, which adapts to the short time periods. Compared to SLR, the maximum transmission capacity can be adjusted according to the ambient temperature and weather conditions changes in RTM when using DLR.

PTDF correction improves the accuracy of power flow distribution and dynamic line rating further reduces the relatively conservative dispatch margin. Both improved methods can regulate network constraints dynamically to fit the instantaneous changes in RTM. Thus, the proposed model increases the line utilization rate and ensures the safe operation of the power grid. The clearing model can also improve the renewables accommodation effectively due to the accuracy in power dispatch and the adaptability to power fluctuations, which upgrades overall social welfare. More refined models and adaptability to complex systems with various weather conditions will be analyzed in future work.

## REFERENCES

[1] Chen, X., Liu, Y., Wang, Q., Lv, J., Wen, J., Chen, X., ... & McElroy, M. B. (2021). Pathway toward carbon-neutral electrical systems in China by mid-century with negative CO2 abatement costs informed by high-resolution modeling. *Joule*, 5(10), 2715-2741.

[2] H. Chen, *Power grid operation in a market environment: economic efficiency and risk mitigation*: John Wiley & Sons, 2016.

[3] W. Yi, Z. Tao, Z. Yuxin, L. En, C. Xinyu, and W. Jinyu, "Preliminary Study on Capacity Compensation Mechanism Adapted to Development of Electricity Spot Market in China [J]," *Joumal of Electric Power Science and Technology*, vol. 45, no. 6, pp. 1–3, 2021.

[4] A. L. Ott, "Experience with PJM market operation, system design, and implementation," *IEEE Transactions on Power Systems*, vol. 18, no. 2, pp. 528–534, 2003.

[5] A. Sweeting, "Market power in the England and Wales wholesale electricity market 1995-2000," *The Economic Journal*, vol. 117, no. 520, pp. 654–685, 2007.

[6] F. Li and R. Bo, "DCOPF-based LMP simulation: algorithm, comparison with ACOPF, and sensitivity," *IEEE Transactions on Power Systems*, vol. 22, no. 4, pp. 1475–1485, 2007.

[7] M. Nick, O. Alizadeh-Mousavi, R. Cherkaoui, and M. Paolone, "Security constrained unit commitment with dynamic thermal line rating," *IEEE Transactions on Power Systems*, vol. 31, no. 3, pp. 2014–2025, 2015.

[8] L. Da Silva and J. G. de Carvalho Costa, "Transmission loss allocation: I. Single energy market," *IEEE Transactions on Power Systems*, vol. 18, no. 4, pp. 1389–1394, 2003.

[9] B. Eldridge, R. O'Neill, and A. Castillo, "An improved method for the DCOPF with losses," *IEEE Transactions on Power Systems*, vol. 33, no. 4, pp. 3779–3788, 2017.

[10] E. Litvinov, T. Zheng, G. Rosenwald, and P. Shamsollahi, "Marginal loss modeling in LMP calculation," *IEEE Transactions on Power Systems*, vol. 19, no. 2, pp. 880–888, 2004.

[11] B. Eldridge, R. P. O'Neill, and A. Castillo, "Marginal loss calculations for the DCOPF," *Federal Energy Regulatory Commission, Tech. Rep,* 2017.

[12] X. Cheng and T. J. Overbye, "PTDF-based power system equivalents," *IEEE Transactions on Power Systems*, vol. 20, no. 4, pp. 1868–1876, 2005.

[13] Z. Yang, H. Zhong, A. Bose, T. Zheng, Q. Xia, and C. Kang, "A linearized OPF model with reactive power and voltage magnitude: A pathway to improve the MW-only DC OPF," *IEEE Transactions on Power Systems*, vol. 33, no. 2, pp. 1734–1745, 2017.

[14] C.-M. Lai and J. Teh, "Comprehensive review of the dynamic thermal rating system for sustainable electrical power systems," *Energy Reports*, vol. 8, pp. 3263–3288, 2022.

[15] D. A. Douglass and A.-A. Edris, "Field studies of dynamic thermal rating methods for overhead lines," in *1999 IEEE Transmission and Distribution Conference (Cat. No. 99CH36333)*, 1999, pp. 842–851.

[16] L. Rácz and B. Németh, "Dynamic line rating—An effective method to increase the safety of power lines," *Applied Sciences*, vol. 11, no. 2, p. 492, 2021.

[17] M. Tschampion, M. A. Bucher, A. Ulbig, and G. Andersson, "N-1 security assessment incorporating the flexibility offered by dynamic line rating," in *2016 Power Systems Computation Conference (PSCC)*, 2016, pp. 1–7.

[18] M. A. Bucher and G. Andersson, "Robust corrective control measures in power systems with dynamic line rating," *IEEE Transactions on Power Systems*, vol. 31, no. 3, pp. 2034–2043, 2015.

[19] N. Viafora, S. Delikaraoglou, P. Pinson, and J. Holbøll, "Chance-constrained optimal power flow with non-parametric probability distributions of dynamic line ratings," *International Journal of Electrical Power & Energy Systems*, vol. 114, p. 105389, 2020.

[20] M. Wang, M. Yang, J. Wang, M. Wang, and X. Han, "Contingency analysis considering the transient thermal behavior of overhead transmission lines," *IEEE Transactions on Power Systems*, vol. 33, no. 5, pp. 4982–4993, 2018.

[21] H. Park, Y. G. Jin, and J.-K. Park, "Stochastic security-constrained unit commitment with wind power generation based on dynamic line rating," *International Journal of Electrical Power & Energy Systems*, vol. 102, pp. 211–222, 2018.

[22] C. Wang, R. Gao, F. Qiu, J. Wang, and L. Xin, "Risk-based distributionally ronodet optimal power flow with dynamic line rating," *IEEE Transactions on Power Systems*, vol. 33, no. 6, pp. 6074–6086, 2018.

[23] M. A. Mohamed, E. M. Awwad, A. M. El-Sherbeeny, E. A. Nasr, and Z. M. Ali, "Optimal scheduling of reconfigurable grids considering dynamic line rating constraint," *IET Generation, Transmission & Distribution*, vol. 14, no. 10, pp. 1862–1871, 2020.

[24] A. Kirilenko, M. Esmaili, and C. Y. Chung, "Risk-Averse Stochastic Dynamic Line Rating Models," *IEEE Transactions on Power Systems*, 2020.

[25] Y. Bai et al., "Improved Spot Market Clearing model based on DC Power Flow Model Based With PTDF Corrections," in *2021 IEEE 4th International Electrical and Energy Conference (CIEEC)*, 2021, pp. 1–5.

[26] J. Peschon, D. S. Piercy, W. F. Tinney, and O. J. Tveit, "Sensitivity in power systems," *IEEE Transactions on Power Apparatus and Systems*, no. 8, pp. 1687–1696, 1968.

[27] H. B. Sun and B. M. Zhang, "A systematic analytical method for quasi-steady-state sensitivity," *Electric Power Systems Research*, vol. 63, no. 2, pp. 141–147, 2002.

[28] IEEE Std. 738-2006—IEEE Standard for Calculating the Current-Temperature of Bare Overhead Conductors, 2007.

[29] "The thermal behavior of overhead line conductors," Cigre Working Group 22. 12, 1992.

[30] J. Teh, C.-M. Lai, and Y.-H. Cheng, "Impact of the real-time thermal loading on the bulk electric system reliability," *IEEE Transactions on Reliability*, vol. 66, no. 4, pp. 1110–1119, 2017.

[31] J. Teh, "Uncertainty analysis of transmission line end-of-life failure model for bulk electric system reliability studies," *IEEE Transactions on Reliability*, vol. 67, no. 3, pp. 1261–1268, 2018.

[32] B. Jimada-Ojuolape and J. Teh, "Impacts of Communication Network Availability on Synchrophasor-Based DTR and SIPS Reliability," *IEEE Systems Journal*, 2021.

[33] B. Jimada-Ojuolape and J. Teh, "Composite Reliability Impacts of Synchrophasor-Based DTR and SIPS Cyber-Physical Systems," *IEEE Systems Journal*, 2022.

[34] M. K. Metwaly and J. Teh, "Fuzzy dynamic thermal rating system-based SIPS for enhancing transmission line security," *IEEE Access*, vol. 9, pp. 83628–83641, 2021.

**Hongyu Pan** received the B.S. degree in electrical engineering from Huahzong University of Science and Technology (HUST), Wuhan, China, in 2021.

He is currently working toward the M.D. degree in electrical engineering with HUST, Wuhan, China. His research interests include power system dispatch and electricity market.

**Xinyu Chen** (M'14) received the B.S. and Ph.D. degrees in electrical engineering from Tsinghua University, Beijing, China, in 2009 and 2014, respectively.

He was an exchange Ph.D. student with Harvard University in 2012, where he was a Postdoctoral Researcher from 2015 to 2016. Since 2016, he has been a Lecturer with Harvard University. He is currently a Professor with the School of Electrical and Electronic Engineering, Huazhong University of Science and Technology, Wuhan, China. He has published over 50 papers on journals, including *Nature Energy*, *Joule* and *Science Advances*. His research interests include power system operation and planning, multi-energy system optimization, renewable energy integration and energy policy.

**Tianyu Jin** (S'21) received the B.S. degree in electrical engineering from Huahzong University of Science and Technology (HUST), Wuhan, China, in 2020.

He is currently working toward the Ph.D. degree in electrical engineering with HUST, Wuhan, China. His research interests include integrated energy system, peer-to-peer energy trading, and electricity market.

**Yang Bai** is with Guangdong Power Grid Co., Ltd Power Dispatch and Control Center Guangdong, China.

**Zhongfei Chen** is with Guangdong Power Grid Co., Ltd Power Dispatch and Control Center Guangdong, China.

**Jinyu Wen** (Member, IEEE) received the B.Eng. and Ph.D. degrees all in electrical engineering from the Huazhong University of Science and Technology (HUST), Wuhan, China, in 1992 and 1998, respectively. He was a Visiting Student from 1996 to 1997 and a Research Fellow from 2002 to 2003 all with the University of Liverpool, U.K., and a Senior Visiting Researcher with the University of Texas at Arlington, USA, in 2010. From 1998 to 2002, he was a Director Engineer in XJ Electric Company Ltd., in China. In 2003, he joined the HUST and currently is a Professor with HUST. His current research interests include renewable energy integration, energy storage application, dc grid, and power system operation and control.

**Qiuwei Wu** (Senior Member, IEEE) received the Ph.D. degree in power system engineering from Nanyang Technological University, Singapore, in 2009. He is currently an Associate Professor with the Department of Electrical Engineering, Technical University of Denmark, Kongens Lyngby, Denmark. His research interests include operation and control of power systems with high penetration of renewables, including wind power modelling and control, active distribution networks, and operation of integrated energy systems.